Enhancement of Catalytic Activity for Toluene Disproportionation by Loading Lewis Acidic Nickel Species on ZSM-5 Zeolite

Satoshi Suganuma*[1], Koshiro Nakamura[2], Akihito Okuda[2], and Naonobu Katada[2]

1 Center for Research on Green Sustainable Chemistry, Graduate School of Engineering, Tottori University, 4-101 Koyama-cho Minami, Tottori 680-8552, Japan

2 Department of Chemistry and Biotechnology, Graduate School of Engineering, Tottori University, 4-101 Koyama-cho Minami, Tottori 680-8552, Japan

* E-mail: suganuma@chem.tottori-u.ac.jp, Tel.: +81 (857) 31-5256, Fax: +81 (857) 31-5684

Abstract

Impregnation of various heteroelements on the ZSM-5 zeolite was applied to improvement of the catalytic activity in toluene disproportionation. Nickel loaded on ZSM-5 (Ni/ZSM-5) exhibited higher catalytic activity (toluene conversion) and lower benzene / xylene ratio (closer to the stoichiometry, meaning low rate of side reaction) than H-ZSM-5 zeolite. The Ni/ZSM-5 with Ni/Al = 0.6 showed the maximum in catalytic activity, and excess Ni loading caused decrease in the conversion and increase in the benzene / xylene ratio due to decrease of acid amount and acceleration of dealkylation, respectively. The detailed analysis of acidic property by means of

ammonia IRMS-TPD method showed that the Ni loading generated Lewis acid sites on the zeolite. The synergy of Brønsted and Lewis acid sites, ascribed to Si-OH-Al and Ni species, respectively, is suggested to give the high activity of desired reaction.

Keywords

ZSM-5, Ni loading, toluene disproportionation, acidic property, synergy effect

1. Introduction

Para-xylene is one of the most valuable aromatic compounds, because it is the raw material of polyethylene terephthalate. The selective formation of *para*-xylene is performed in the toluene disproportionation (Scheme S1 in the supporting information), as well as the alkylation of toluene with methanol, the transalkylation of methylbenzene derivatives and xylene isomerization. In toluene disproportionation, a ZSM-5 zeolite with the micropores whose size is similar to the benzene ring is utilized as a catalyst forming *para*-xylene selectively [1,2]. Recent studies concerns with the modification of ZSM-5 to improve the selectivity of *para*-xylene, including impregnation of P, Mg, B and La [3-5], pre-coking [6,7], chemical vapor deposition (CVD) [8,9], chemical liquid deposition (CLD) of silica [10-12], and silicalite coating [13]. The selectivity of *para*-xylene 93% in the C8 aromatic compounds at 30% of the toluene conversion in

the industrial process has been achieved [14]; the selectivity is usually decreased with increasing the conversion by varying the reaction conditions on one catalyst, and therefore the high selectivity at a certain high level of conversion is demanded. The 99.8% selectivity at 10.9% of the conversion have been achieved in laboratory [15]. Further improvement of the catalyst available to industrial process is strongly demanded, because the energy-consuming separation step after the reaction can be omitted with such a high selectivity over 99.7 %. Two alternatives can be proposed to realize the high performance, (1) suppression of the undesired reaction presumably due to heterogeneous pore-opening size, or (2) enhancing the catalytic activity of zeolite. Attempts from the former viewpoint have been carried out based on various techniques [6-13]. The present study focuses on the latter concept. Modification of the active sites in the ZSM-5 is attempted to increase the activity.

In this study, we selected the sample of ZSM-5 (MFI structure) with the practically highest Al concentration (SiO_2 / Al_2O_3 = 23.8) as the parent zeolite because of the following reasons. (1) The MFI structure possessed the shape selectivity in toluene disproportionation. (2) The active species for this reaction has been generally considered to be Brønsted acid site [10]. The number of Brønsted acid sites on zeolites is principally equal to the number of Al atoms [16].

In the present study, we introduced various heteroelements on the ZSM-5 zeolite to improve the catalytic activity, because this method was assumed to keep the pore structure of the zeolite. We investigated the catalytic activity and the reaction mechanism for the toluene disproportionation of heteroatoms supported on ZSM-5 with the high Al concentration.

2. Experimental

A Na/ZSM-5 (Tosoh, SiO_2 / Al_2O_3 = 23.8) zeolite was ion-exchanged into NH_4-ZSM-5 in an 5 wt.% ammonium nitrate solution (NH_4 / Na in the system = 10) at 353 K for 4 h, then filtrated and washed with water 3 times. These procedures (stirring, filtrating and washing) were repeated 3 times. The zeolite finally was dried at 373 K for 12 h. The thus obtained NH_4-form zeolite was employed as the parent zeolite in the following modification procedures without converting it into the proton form, because it has been known that proton form zeolites can be dealuminated by water vapor in atmosphere [17,18].

The introduction of nickel and other metals were typically performed by means of an impregnation method. 100 mL of aqueous nitrate solution of the metal elements were impregnated on 5.0 g of NH_4-ZSM-5 with stirring at 353 K. Then, the solvent

was dried at 373 K for 12 h in air. The yielded solid is named Ni-*x* where *x* is the Ni/Al molar ratio based on the composition of impregnated solution; the metal to Al ratio was fixed at 0.6 in the cases of other metals. A Ni/SiO_2 catalyst with 6.1 wt% of Ni was also prepared by the same method using a silica gel support (Reference Catalyst, Catalysis Society of Japan, JRC-SIO-10). As a comparison, a sample of Ni/ZSM-5 was prepared by means of an ion exchange method. After the ZSM-5 zeolite was put into an aqueous solution of nickel nitrate and stirred at 353 K for 4 h, the solid was filtered and dried at 373 K for 12 h in air. The yielded solid is named Ni-*x*(EX) where *x* is the Ni/Al molar ratio based on the composition of employed solution, and the actual composition was measured by ICP as described later.

The crystal structure was characterized by X-ray diffraction (Rigaku, Ultima IV), inductively coupled plasma-atomic emission spectrometry (Rigaku, ICP CIROS), and N_2 adsorption (Microtrac BEL, BELSORP-MAX). The adsorption isotherms was measured at 77 K after pretreatment at 573 K, and the surface area and the pore volume were calculated based on BET (Brunauer-Emmett-Teller) equation, BJH (Barrett-Joyner-Halenda), and t-plot methods.

Ammonia IRMS-TPD analysis [19] was carried out using an automatic IRMS-TPD analyzer (MicrotracBEL). Powder of Ni/ZSM-5 was compressed into a

self-supporting disk with 1 cm of the diameter under 20 MPa, and pre-treated in an oxygen flow (37 μmol s^{-1}, 100 kPa) at 823 K for 1 h and a hydrogen flow (7 μmol s^{-1}, 100 kPa) at 773 K for 1 h in an in-situ IR cell. Also NH_4-ZSM-5 was pre-treated in similar way into H-ZSM-5, but the hydrogen treatment was omitted. The sample was heated at a ramp rate of 2 K min^{-1} during the elevation temperature from 343 to 803 K in a helium flow (89 μmol s^{-1}, 6.0 kPa), and an IR spectrum was collected. Then, ammonia was adsorbed at 343 K, and the heating and collecting IR spectra in a helium flow were repeated. The concentration of ammonia in the gas phase was monitored by a mass spectrometer (MS) operating at m/e 16. The amount of acid sites was calculated from the intensity of ammonia desorption in the TPD spectrum. The enthalpy of ammonia desorption (ΔH) was calculated as an index of acid strength from the ammonia desorption profile based on the thermodynamic theory [20].

Nickel on ZSM-5 was characterized by means of IR spectroscopy of adsorbed CO using an automatic IRMS-TPD analyzer (MicrotracBEL). The catalysts was pretreated at 823 K in an oxygen flow and in a hydrogen flow. Then, the IR cell was cooled to 293 K, and evacuated. The background was recorded in evacuation at 293 K. After introduction of CO, the IR cell was evacuated for 15 min. IR spectra in each step was recorded at every predetermined time. The CO adsorption capacity was

analyzed by a volumic gas adsorption analyzer (Microtrac BEL, BELSORP-MAX). The samples were pre-treated in an oxygen flow at 773 K for 1 h and a hydrogen flow at 773 K for 1 h in an in-situ sample tube. CO was adsorbed on the samples at 323 K.

In order to evaluate the activity for the toluene disproportionation, 0.1 g of the catalyst was packed in a stainless steel tube (i.d. 4 mm) and pretreated in H_2 (0.015 mol h^{-1}, 100 kPa) at 773 K for 1 h. In this process, ammonium ion on the zeolite was desorbed, and H(proton)-type zeolite was formed. Then, the catalyst bed was cooled down to 673 K, and the back-pressure valve was adjusted to keep the total pressure at 1.5 MPa. Toluene and H_2 were fed at 0.015 mol h^{-1} for each. The products were trapped by hexane at 273 K and analyzed by a GC (gas chromatograph) with a FID (flame ionization detector). On the other hand, dealkylation (cracking) of cumene (isopropylbenzene, 2-phenylpropane) was carried out by a pulse method in a He flow as described elsewhere [21]. The catalyst (1 mg) was packed in a stainless steel tube (i.d. 4 mm) and pretreated in a He flow (0. 15 mol h^{-1}, 100 kPa) at 773 K for 1 h. Then, a pulse of cumene (28.7 μmol) was fed at 473 K. The outlet gas was analyzed by a GC (gas chromatograph) with a FID (flame ionization detector).

3. Results

3.1. Characterization of Ni/ZSM-5

The structural analyses were applied to Ni/ZSM-5 (Ni-0.6, Ni-1.0 and Ni-2.1) and H-ZSM-5. It is presumed that Ni species before the reaction had been fully oxidized and dispersed on surface, because they were formed from nickel nitrate solution. The pretreatment of reaction was carried out in a flow of H_2, and Ni species should be reduced. Fig. 1 (a) displays X-ray diffraction patterns of the catalysts after the reduction in a flow of H_2 at 773 K for 1 h. The patterns of Ni/ZSM-5 exhibited narrowed and well-defined diffraction peaks similar to those of H-ZSM-5, demonstrating that the crystal structure of MFI structure in the Ni/ZSM-5 were unchanged by the Ni loading and H_2 reduction. Fig. 1 (b) shows an enlarged portion of Fig. 1 (a). The XRD patterns of Ni/ZSM-5 revealed clear additional peaks at 2θ = 44.5º and 51.8º attributable to Ni metal particles, and the peak was especially large on Ni-2.1.

The Ni/Al molar ratios in the catalysts were determined by ICP analysis, as shown in Table 1. The Ni/Al contents in Ni-0.6 and Ni-1.0 prepared by the impregnation method were found to be in generally agreement with the composition of impregnated solutions, indicating that most of Ni was loaded on the support by the impregnation procedure. On the other hand, Ni-0.5(EX) and Ni-0.9(EX) were

prepared by the ion-exchange method, where the zeolite and solution were stirred at the same temperature employed for the impregnation method and then unfixed Ni was washed out. Most of Ni was loaded on Ni-0.5(EX) as confirmed by ICP. However, the ICP analysis for Ni-0.9(EX) indicated that only 0.56 of Ni relative to Al was exchanged while 0.90 of Ni was employed. In other words, the ion exchange capacity of Ni on this NH_4-ZSM-5 in these conditions was about a half of Al content. This suggests that the valence of Ni was two during the ion exchange procedure. The employed H-ZSM-5 (SiO_2 / Al_2O_3 = 23.8) had 1.29 mol kg^{-1} of Al and 6.1 wt% of nickel represented 1.04 mol kg^{-1}, considering that nickel (Ni^{2+}) could undergoes exchange in one or two acid sites. This means that 4.2 wt% is the superior limit for exchange nickel. For instance Ni-0.9(EX) and Ni-0.5(EX) show similar Ni/Al ratio.

As shown in Fig. 2, N_2 adsorption-desorption isotherms of the investigated samples were of type I, evidencing a microporous texture. In addition, presence of the slope at P/P_0 = 0.4 - 1 (clearly shown by the presence of hysteresis loop) in the each isotherm suggests mesoporous feature. The uptake at P/P_0 close to zero was almost unchanged by the Ni loading, consistent with the microporous structure was not modified by the Ni impregnation procedure. Surface area of micropore and larger pore wall remained approximately invariable (Fig. S1). Pore volume of micropore was the

same in the catalysts, while that of mesopore increased by Ni loading (Fig. S2).

The acidic properties of Ni/ZSM-5 and H-ZSM-5 were analyzed by a method of ammonia infrared-mass spectroscopy / temperature-programmed desorption (IRMS-TPD). This method can determine the number, strength (enthalpy or energy of ammonia desorption) and type (Brønsted or Lewis) of acid sites on a solid [16]. Fig. 3 shows enlarged portions of difference IR spectra obtained on the zeolites at 373-773 K during the TPD experiments. A sharp band at ca. 1450 cm^{-1} was assigned to bending (ν_4) vibration of NH_4^+ adsorbed on Brønsted acid sites (NH_4B). This band was observed even after the loading of Ni with more than 2 of the Ni/Al ratio, demonstrating that a fraction of Brønsted acid sites were not interacted with Ni cation. It is supposed that the impregnated Ni^{2+} species were partially transformed in the process of pretreatment (reduction by H_2) into metal particle which indirectly or not interacted with the support, and therefore Brønsted acid site was regenerated. A small peak at ca. 1622 cm^{-1} was attributed to δ_d of NH_3L (NH_3 coordinated to Lewis acid sites) [20]. On pure aluminosilicates with Lewis acidity due to Al species, a stronger vibration mode (δ_s) is observed at 1250-1330 cm^{-1}, and the intensity changes against the temperature of δ_d and δ_s are similar, because these bands are two different modes of one compound. The amount of NH_3L (ammonia coordinated to Lewis acidic Al species in the case of

aluminosilicate) was calculated from the IR-TPD of δ_s, in order to minimize the error utilizing the more intense band [19]. However, the intensities of δ_d and δ_s are not consistent in Ni/ZSM-5, suggesting the presence of hidden band of δ_s. It is considered that the band of δ_s on Ni/ZSM-5 had a lower wavenumber than that on aluminosilicate, and was thus overlapped by the skeletal vibration of zeolites; it is reasonable that the NH_3-Ni species has a different vibration frequency from that of NH_3-Al. The amount of NH_3L was determined from IR-TPD of δ_d. The peak ascribed to NH_3L was not observed in the spectra of H-ZSM-5 (Fig. 3 (a)), and the loading of Ni created Lewis acid sites (Fig. 3 (b)-(d)). The peak around 1680 cm^{-1} in all the spectra was ascribed to the δ_s vibration of NH_3 hydrogen-bonded [19].

Fig. 4 shows TPD profiles of ammonia desorbed from the acid sites. MS-TPD indicates the profile of NH_3 desorption evaluated with mass spectroscopy. The TPD profiles of NH_4B and NH_3L were calculated from the IR-TPD of ca. 1450 cm^{-1}-band (ν_4, NH_4) and ca. 1622 cm^{-1}-band (δ_d, M-NH_3), respectively. MS-TPD was assumed to be the sum of TPD profiles for NH_4B and NH_3L, while the peak around 410 K was ascribed to NH_3 hydrogen-bonded and was not contained as species adsorbed on acid sites. Table 2 lists the acid amount and average enthalpy upon NH_3 desorption (ΔH, index of acid strength) calculated from the TPD profiles. It was found that the loading

of Ni decreased the Brønsted acid sites and increased the amount of Lewis acid sites. The strength (ΔH) of Brønsted acid sites slightly declined by Ni-loading. On the other hand, average ΔH of Lewis acid sites cannot appropriately calculated, because TPD profiles for NH_3L were much broader than those for NH_3B.

Many researchers reported CO adsorption on different nickel species, and especially Hadjiivanov et.al. studied FTIR analysis of CO adsorption on Ni/ZSM-5 [22] and Ni/SiO_2 [23]. CO adsorbed on oxidized Ni/ZSM-5 was mainly bonded with Ni^{2+} by a σ bonding [22]. After reduction of Ni/ZSM-5, a fraction of nickel species were changed into Ni^{+}, which were bonded with CO by π-back bonding [22]. CO bonded with acidic hydroxyls on zeolite was also detected on Ni/ZSM-5 [22]. CO adsorbed on reduced Ni/SiO_2 was characterized as polycarbonyl coordinated with nickel metal [23]. In our study, the samples were pretreated in flow of hydrogen at 773 K, and then cooled to 293 K. The background spectrum was recorded in evacuation. After introduction of CO (about 3 kPa equilibrium pressure), CO was evacuated for 15 minutes. Fig. S3 shows IR spectra in the process of CO desorption on the catalysts. The wavenumber of the stretching vibration of CO gas is 2143 cm^{-1}. In Fig. S3 (a), the bands at 2170 and 2121 cm^{-1} were assigned to H-bonded CO and physically adsorbed CO on H-ZSM-5, respectively. The bands at 2209 and 2054 - 2050 cm^{-1} on Ni-0.6 and Ni-1.0

(Fig. S3 (b) and (c)) were also observed, and assigned to monocarbonyl of Ni^{2+} - CO type [22] and tetracarbonyl of Ni^0 $(CO)_4$ type [23]. The weak bands at 2100-2090 and 2003 cm^{-1} may be assignable to $Ni(CO)_4$ of defect sites and Ni^0 $(CO)_x$ (x < 4), respectively. Namely, CO introduced into Ni-0.6 and Ni-1.0 was adsorbed on Ni^{2+}, Ni^0 metal, and acidic hydroxyl group. In Fig. S3 (d), CO introduced into Ni-2.1 was adsorbed on Ni^0 metal and acidic hydroxyl group. The shoulder band at 2087 cm^{-1} may be assignable to $Ni(CO)_4$ of defect sites, and the broad band at 1901 cm^{-1} was speculated to be assigned to $Ni^0{}_x(CO)$ (x > 1) [23]. Nickel on Ni-2.1 is not Ni^{2+} but Ni^0 metals, which aggregate speculatively. It was revealed that the low content of Ni on the catalyst kept oxidation state of nickel. Fig. S4 shows amount of adsorbed CO at 323 K. The large amount of loading nickel (Ni / Al > 0.6) leaded gradual increase in the amount of adsorbed CO.

3.2. Catalytic activity for toluene disproportionation

Various transition metals were introduced into ZSM-5 at 0.6 of the metal/Al atomic ratio by the impregnation method. The catalytic activities of the ZSM-5 zeolites with different metals for toluene disproportionation were recorded, as shown in Fig. S5, which compares the initial catalytic activity, represented by the conversion at

75 min of the time on stream (the initial products were collected between 45 – 75 min, because the influent could not be obtained in the trap tube between 0 – 45 min). In this reaction, main products were xylene isomers and benzene. Little other products containing ethylbenzene were detected in FID–GC analysis. The loading of Ni increased the initial activity by 1.6 times against H-ZSM-5, whereas the other elements decreased the activity.

Fig. 5 (a) compares the activities for the toluene disproportionation over Ni/ZSM-5 with various Ni contents; the Ni content is based on the composition of impregnated solution, and this value has been confirmed by ICP to be approximately same to the Ni content in the solid. The activity increased with the loading in 0 - 1 of the Ni/Al ratio, and showed the maximum at 1.0 of the Ni/Al ratio. However, excess Ni gave decrease in the activity. The catalytic activity of Ni/SiO_2 containing the Ni content (6.1 wt%) same to that of Ni-1.0 is shown in Table 3; Ni/SiO_2 exhibited lower conversion than Ni-1.0, but higher than H-ZSM-5 (Ni/Al = 0).

The disproportionation of toluene into benzene and xylene should result in unity of the benzene / xylene molar ratio according to the stoichiometry (Scheme S1). The yield of xylene isomers generally showed 26 % *p*-xylene, 53 % *m*-xylene and 21 % *o*-xylene, which are same to the ratios of equilibrium mixture of xylenes. In this study,

1 the shape selectivity was not found as observed on H-ZSM-5 zeolite at a high
2 conversion of toluene without catalyst modification techniques [3-13]. Fig. 5 (b)
3 shows the relationship between the benzene / xylene ratio and Ni content on the ZSM-5
4 support. The benzene / xylene ratio was around 1 at Ni/Al < 1 and increased with
5 loading of excess Ni. The high benzene / xylene ratio indicates the side reaction such
6 as dealkylation of toluene and alkylbenzene (e.g., ethylbenzene). In detail, the
7 benzene / xylene ratio was slightly higher than 1 (ca. 1.2) at Ni/Al = 0 and obviously
8 decreased with Ni loading up to Ni/Al = 0.6. On the other hand, Ni/SiO_2 showed an
9 obviously high value, 14.3, of the benzene / xylene ratio in the same reaction conditions,
10 suggesting that the Ni^0 particle on Ni/SiO_2 generated high dealkylation activity.
11 Fig. 6 shows the catalytic activity for cumene cracking, which has been utilized
12 as a test reaction of solid acid catalyst. It also revealed the maximum at 1.0 of the
13 Ni/Al ratio, similarly to the toluene disproportionation. These suggest that the Ni/Al
14 ratio 1 was effective in the enhancement of activity, and the excess Ni induced drastic
15 decline of the catalytic activity.
16 Fig. 7 (a) shows the toluene conversion as a function of time on stream in the
17 toluene disproportionation. Besides the activity change by Ni loading stated above,
18 the conversion of Ni loaded on ZSM-5 zeolites and Ni/SiO_2 was gradually decreased

with the time on stream, and showed a plateau over 240 min. The catalytic activities of Ni-0.6 and Ni-1.0 even after decline exhibited higher than that of H-ZSM-5. On the other hand, Ni/SiO_2 and Ni-2.1 seems to have very high initial activity but showed relatively fast decrease of the conversion. Ni-0.6 exhibited comparable stability to H-ZSM-5. Fig. 7 (b) compares the benzene/xylene molar ratio as a function of the time on stream. As already stated, Ni-0.6 showed the benzene / xylene ratio lower than that on H-ZSM-5. The benzene/xylene ratios for Ni/SiO_2 showed >13.0 over the time on stream in the present experiments (data not shown).

4. Discussion

4.1. Characterization

According to Maia et al. [24], Ni-ZSM-5 prepared by impregnation and calcination in air has three types of nickel species; NiO particle, nickel oligomeric species in the zeolite channels, and nickel species as the counter cations of ion exchange sites in the zeolite framework. In the TPR (temperature-programmed reduction) profiles, nickel species in NiO particle are reduced at temperature lower than those required for reducing nickel oligomeric species in the zeolite channels. It is considerably difficult to reduce nickel species as counter cations in the zeolite

framework.

The chemical compositions of ion exchanged samples suggested that the ion exchange capacity of the employed ZSM-5 was about a half of Al content at 353 K, the temperature commonly adopted to the ion exchange and impregnation methods, presumably because that Ni was divalent. It implies that most of Ni species on Ni-0.6 were the counter cations of ion exchange sites (hereafter counter cation); the pretreatment of reaction may reduce all or a part of them, but anyway, finely dispersed Ni species were presumably formed on Ni-0.6, simultaneously the Brønsted acid sites were reproduced. In the ICP analysis (Table 1), it indicates that 0.56 – 0.57 of Ni relative to Al can be loaded on the zeolite. In the impregnation process, most of Ni species should be divalent and loaded as the counter cations of two ion exchange sites. However, all ion exchange sites on the ZSM-5 zeolite do not possess adjacent another ion exchange sites. The isolated site may possess one Ni counter cation, which cause that ion-exchange capacity by Ni is 0.56 – 0.57. On the contrary, it is speculated that the surplus of Ni preferentially formed oligomeric species in the zeolite channels in the cases where the amount of such Ni species was small. It is therefore considered that Ni-0.6 mainly possessed the counter cations-originated species, whereas Ni-1.0 had both of the counter cations-originated species and the oligomerized species in zeolite

channels. The driving force of dispersion of these species should be the presence of ion exchange sites and microporous nature, and therefore most of Ni species in these samples are considered to be located in the micropores nearby acidic OH groups (ion exchange sites). On the contrary, excess Ni should be weakly attached to the surface in the cases of impregnation method, and therefore it is speculated that relatively large fractions of Ni in Ni-2.1 formed particles on the external surface as aggregates. Nickel in Ni/SiO_2 was probably reduced into Ni particle far larger than atomic scale.

As shown in Table 2, the loading of Ni up to 1 of Ni/Al ratio decreased the Brønsted acid sites and increased the amount of Lewis acid sites. Therefore, the modification of acidic property by Ni loading can be summarized as follows: [i] Brønsted acid site was decreased by ion exchange with Ni species, and [ii] Lewis acid sites were generated on relatively small Ni particles dispersed in the zeolite channels.

4.2. Catalytic activity

The enhancement of activities for both reactions (cumene cracking and toluene disproportionation) is considered to be due to generation of the nickel species and some changed of Brønsted acidic nature of ZSM-5. In toluene disproportionation, the activity was found to be increased with loading of Ni up to 1 of Ni/Al ratio, suggesting

that co-presence of the relative dispersed Ni species in the zeolite channels and the ion-exchange sites generated the activity. Benzene / xylene ratio of Ni-0.6 showed close to 1, which was lower than that of Ni-0.5. The appropriate loading amount was 0.6.

In contrast, the excess Ni loaded on the ZSM-5 zeolite (Ni/Al > 1.0) is considered to catalyze side reaction and show high benzene/xylene ratio, as well as that on the silica gel. It suggests that the reduced Ni species derived from NiO particle in Ni/SiO_2 have intrinsically high conversion of toluene and benzene / xylenes ratio. Fast deactivation was observed on Ni-2.1 and Ni/SiO_2. These are reasonably consistent with each other, because the side reaction forming benzene and alkenes should increase the benzene / xylene ratio and simultaneously increase the rate of coke formation from alkenes, resulting in the catalyst deactivation. The appropriate amount of Ni loading to form the Ni species dispersed in the zeolite channels to keep the synergy with ion exchange sites is believed to enhance the catalytic activity for toluene disproportionation, and improved the xylene selectivity.

4.3. Reaction mechanism

Some preceding studies proposed the reaction mechanisms of toluene

disproportionation based on the experimental observations (Scheme S2) [25-27]. The mechanism drawn in Scheme S2 [26] proceeds through hydride abstraction followed by the formation of diphenyl methane; these steps were accelerated by Brønsted and Lewis acid sites.

This study suggested that the Ni-0.6 sample possessed Ni species as counter cations (-ONi) in the micropores and showed high catalytic activity and stoichiometric formation of xylene and benzene (1:1). It can be explained that Lewis acid sites derived from –ONi species and the Brønsted acid site on the zeolite worked concertedly to have synergy effect for the toluene disproportionation. Mavrodinova et al. [28] have suggested that the reactivity of HY zeolite modified with InO^+ was different from a simply Brønsted acidic zeolite, because Lewis acidic InO^+ species lead a faster hydride abstraction and benzylic cation formation upon toluene and ethylbenzene disproportionation. Recently, it was reported that Pd [29-31] and Ga [32] anchored on ion-exchange sites of ZSM-5 zeolites generate Lewis acid sites, which act for C-H activation and hydride abstraction. It is probable that the toluene disproportionation for Ni-0.6 proceed with the hydride abstraction enhanced by -ONi as Lewis sites and effective transformation of diphenylmethane-like intermediate by Brønsted acid sites (Scheme S2), resulting in the high toluene conversion and benzene / xylene ratio ≈ 1.

This hypothesis is supported by the preceding reports [24,33] that the Ni on Ni/ZSM-5 accelerated dehydrogenation in paraffin cracking.

Ni particles on Ni-2.1 and Ni/SiO_2 brought about faster toluene conversion than Brønsted acid sites on H-ZSM-5, as shown in Table 3. It is proposed that Ni/SiO_2 catalyzed side reactions with dealkylation of alkylbenzenes and coking, and hence to result in the rapid catalyst deterioration, as shown in Fig. 7 (a).

In this study, the activity of ZSM-5 zeolite for the toluene disproportionation was enhanced by simple impregnation of Ni in mild conditions with keeping the textual properties, unlike hydrothermal treatment. It is expected that combination of this method and techniques for improvement of *para*-xylene selectivity with control of fine structure which have been developed [10-13, 33] will open a new way to design a catalyst with high selectivity and activity for *para*-xylene production.

5. Conclusions

The loading of Ni on ZSM-5 increased the catalytic activity for toluene disproportionation and cumene cracking. The formed benzene / xylene ratios in toluene disproportionation was improved into nearby 1.0 by the Ni loading content at Ni/Al = 0.6 on ZSM-5. The MFI crystal structure did not collapse during the Ni

loading. The loading at Ni/Al = 0.6 formed the nickel species as counter cations and Lewis acid sites after the pretreatment in an H_2 flow. Excessive Ni introduction on the zeolite and loading of Ni on a silica gel generated coarse Ni particles. The high toluene conversion and the selective xylene for Ni-0.6 were supposed to be ascribed to the synergy effect of Brønsted acid sites and Lewis acid sites.

References

[1] Y.Y. Fong, A.Z. Abdullah, A.L. Ahmad, S. Bhatia, Chem. Eng. J. 139 (2008) 172-193.

[2] S. Al-Khattaf, S.A. Ali, A.M. Aitani, N. Žilková, D. Kubička, J. Čejka, Catal. Rev. Sci. Eng. 56 (2014) 333-402.

[3] N.Y. Chen, W.W. Kaeding, F.G. Dwyer, J. Am. Chem. Soc. 101 (1979) 6783-6784.

[4] W.W. Kaeding, C. Chu, L.B. Young, B. Weinstein, S.A. Butter, J. Catal. 67 (1981) 159-174.

[5] Y. Sugi, Y. Kubota, K. Komura, N. Sugiyama, M. Hayashi, J.-H. Kim, G. Seo, Appl. Catal. A 299 (2006) 157-166.

[6] F. Bauer, W.H. Chen, Q. Zhao, A. Freyer, S.B. Liu, Micropor. Mesopor. Mater. 47 (2001) 67-77.

[7] F. Bauer, W.H. Chen, E. Bilz, A. Freyer, V. Sauerland, S.B. Liu, J. Catal. 251 (2007) 258-270.

[8] J.H. Kim, A. Ishida, M. Okajima, M. Niwa, J. Catal. 161 (1996) 387-392.

[9] A.B. Halgeri, J. Das, Catal. Today 73 (2002) 65-73.

[10] J. Čejka, N. Žilková, B. Wichterlova, G. Elder-Mirth, J.A. Lercher, Zeolites 17 (1996) 265-271.

[11] S. Zheng, H. Tanaka, A. Jentys, J.A. Lercher, J. Phys. Chem. B 108 (2004) 1337-1343.

[12] S. Laforge, D. Martin, J.L. Paillaud, M. Gusinet, J. Catal. 220 (2003) 92-103.

[13] D.V. Vu, M. Miyamoto, N. Nishiyama, Y. Egashira, K. Ueyama, J. Catal. 243 (2006) 389-394.

[14] J. S. Beck, D. H. Olson, S. B. McCullen, US Patent 5367099A (1994), to Mobil Oil Corporation.

[15] N. Katada, K. Takeshita, Y. Miyazono, M. Niwa, Y. Araki, Jpn. Patent JP2013-163142A (2013), to Tottori University and Jx Nippon Oil & Energy Corporation.

[16] M. Niwa, N. Katada, K. Okumura, Characterization and Design of Zeolite Catalysts: Solid Acidity, Shape Selectivity and Loading Properties, Springer, Berlin, 2010, p. 29-59.

[17] N. Katada, Y. Kageyama, M. Niwa, J Phys Chem B 104 (2000) 7561-7564.

[18] N. Katada, T. Kanai, M. Niwa, Micropor. Mesopor. Mater. 75 (2004) 61-67.

[19] S. Suganuma, Y. Murakami, J. Ohyama, T. Torikai, K. Okumura, N. Katada, Catal. Lett. 145 (2015) 1904-1912.

[20] M. Niwa, N. Morishita, H. Tamagawa, N. Katada N, Catal. Today 198 (2012) 12-18.

[21] M. Niwa, N. Katada, Y. Murakami, J. Phys. Chem. 94 (1990) 6441-6445.

[22] K. Hadjiivanov, H. Knözinger, M. Mihaynov, J. Phys. Chem. B 106 (2002) 2618-2624.

[23] M. Mihaynov, K. Hadjiivanov, H. Knözinger Catal. Lett. 76 (2001) 59-63.

[24] A.J. Maia, B. Lois, Y.L. Lam, M.M. Pereira, J. Catal. 269 (2010) 103-109.

[25] N. P. Rhodes, R. Rudham, J. Chem. Soc. Faraday Trans. 90 (1994) 809-814.

[26] Y. Xiong, P. G. Rodewald, C. D. Chang, J. Am. Chem. Soc. 117 (1995) 9427-9431.

[27] J. Čejka, B. Wichterlová, Catal. Rev. 44 (2002) 375-422.

[28] V. Mavrodinova, M. Popova, M. R. Mihályi, G. Pál-Borbély, C. Minchev, Appl.

Catal. A 262 (2004) 75-83.

[29] Y. Lou, P. He, L. Zhao, H. Song, Fuel 183 (2016) 396–404.

[30] Y. Lou, J. Ma, W. Hu, Q. Dai, L. Wang, W. Zhan, Y. Guo, X.-M. Cao, Y. Guo, P. Hu, G. Lu, ACS Catal. 6 (2016) 8127–8139.

[31] Y. Lou, P. He, L. Zhao, H. Song, Catal. Commun. 87 (2016) 66–69.

[32] H. Xiao, J. Zhang, X. Wang, Q. Zhang, H. Xie, Y. Hana, Y. Tan, Catal. Sci. Technol., 5 (2015) 4081-4090.

[33] A.J. Maia, B.G. Oliveira, P.M. Esteves, B. Lois, Y.L. Lam, M.M. Pereira, Appl. Catal. A 403 (2011) 58-64.

Table 1 Ni/Al molar ratios in Ni/ZSM-5

Sample	Ni/Al based on the composition of impregnation / ion exchange solution	ICP Ni/Al
Ni-0.5*	0.50	0.57
Ni-1.0*	1.04	1.01
Ni-0.5(EX)**	0.50	0.51
Ni-0.9(EX)**	0.90	0.56

*: Impregnation method. **: Ion exchange method.

Table 2 Acidic properties of Ni/ZSM-5

Sample	Brønsted acid site		Lewis acid site
	Amount / mol kg^{-1}	ΔH [*1] / kJ mol^{-1}	Amount / mol kg^{-1}
H-ZSM-5	1.13	141	0.00
Ni-0.6	0.78	136	0.54
Ni-1.0	0.58	134	0.83
Ni-2.1	0.51	134	0.67

[*1] Average enthalpy upon NH_3 desorption

Table 3 Catalytic activity of various catalysts in toluene disproportionation

Sample	Ni / wt%	Conversion* / %	Benzene / xylene molar ratio*
H-ZSM-5	0	10.8	1.25
Ni-0.6 (Ni/ZSM-5)	3.7	18.3	1.07
Ni-1.0 (Ni/ZSM-5)	6.1	25.5	1.37
Ni-2.1 (Ni/ZSM-5)	12.8	12.3	1.50
Ni/SiO_2	6.1	16.4	14.3

*: At time on stream = 75 min.

Figure captions

Fig. 1 (a) XRD patterns and (b) enlarged portion in 2θ = 40-60º.

Fig. 2 N_2 adsorption-desorption isotherms at 77 K.

Fig. 3 Enlarged portion at bending vibration region (1100 – 2000 cm^{-1}) in difference spectra of IR $A(T)$-$N(T)$ [(spectrum after ammonia adsorption) – (spectrum before ammonia adsorption)] on (a) H-ZSM-5, (b) Ni-0.6, (c) Ni-1.0, and (d) Ni-2.1.

Fig. 4 Fitting of IR- and MS-TPD calculating TPD spectrum of Brønsted acid site on (a) H-ZSM-5, (b) Ni-0.6, (c) Ni-1.0, and (d) Ni-2.1.

Fig. 5 (a) Initial conversion of toluene and (b) benzene / xylene molar ratio in disproportionation of toluene on Ni-promoted ZSM-5.

Fig. 6 Initial conversion in dealkylation of cumene on Ni-promoted ZSM-5.

Fig. 7 (a) Conversion of toluene and (b) benzene / xylene molar ratio as a function of time on stream in disproportionation of toluene by Ni/ZSM-5, H-ZSM-5 and Ni/SiO_2.

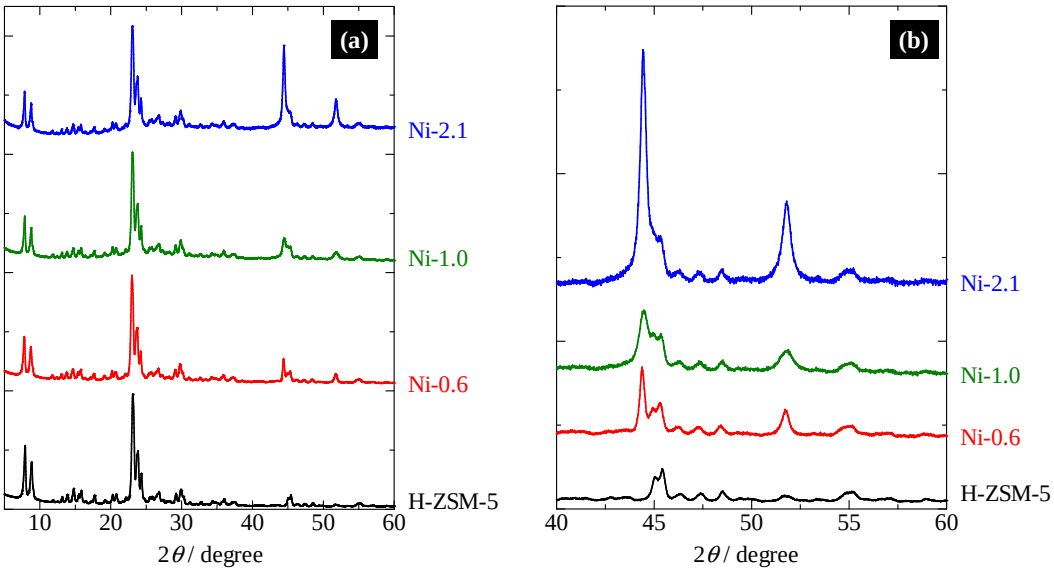
(a)
Ni-2.1
Ni-1.0
Ni-0.6
H-ZSM-5
10
20
30
40
50
60
2θ / degree
(b)
Ni-2.1
Ni-1.0
Ni-0.6
H-ZSM-5
40
45
50
55
60
2θ / degree

Fig. 1

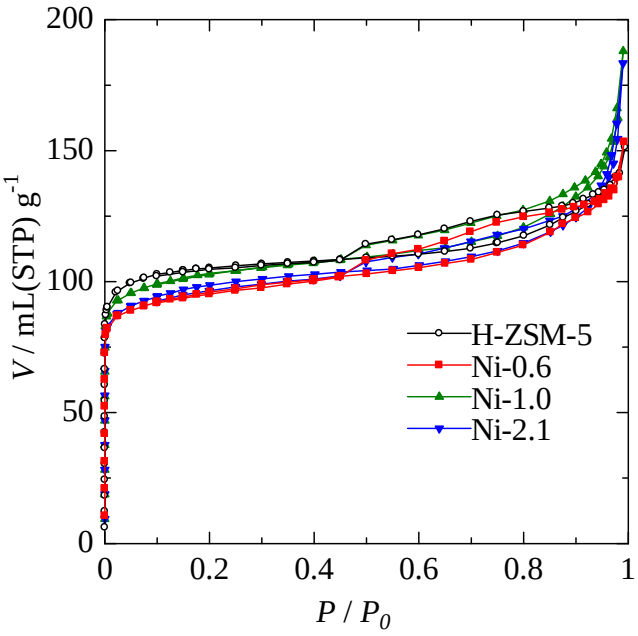
200
150
100
50
0
0
0.2
0.4
0.6
0.8
1
V / mL(STP) g-1
P / P0
H-ZSM-5
Ni-0.6
Ni-1.0
Ni-2.1

Fig. 2

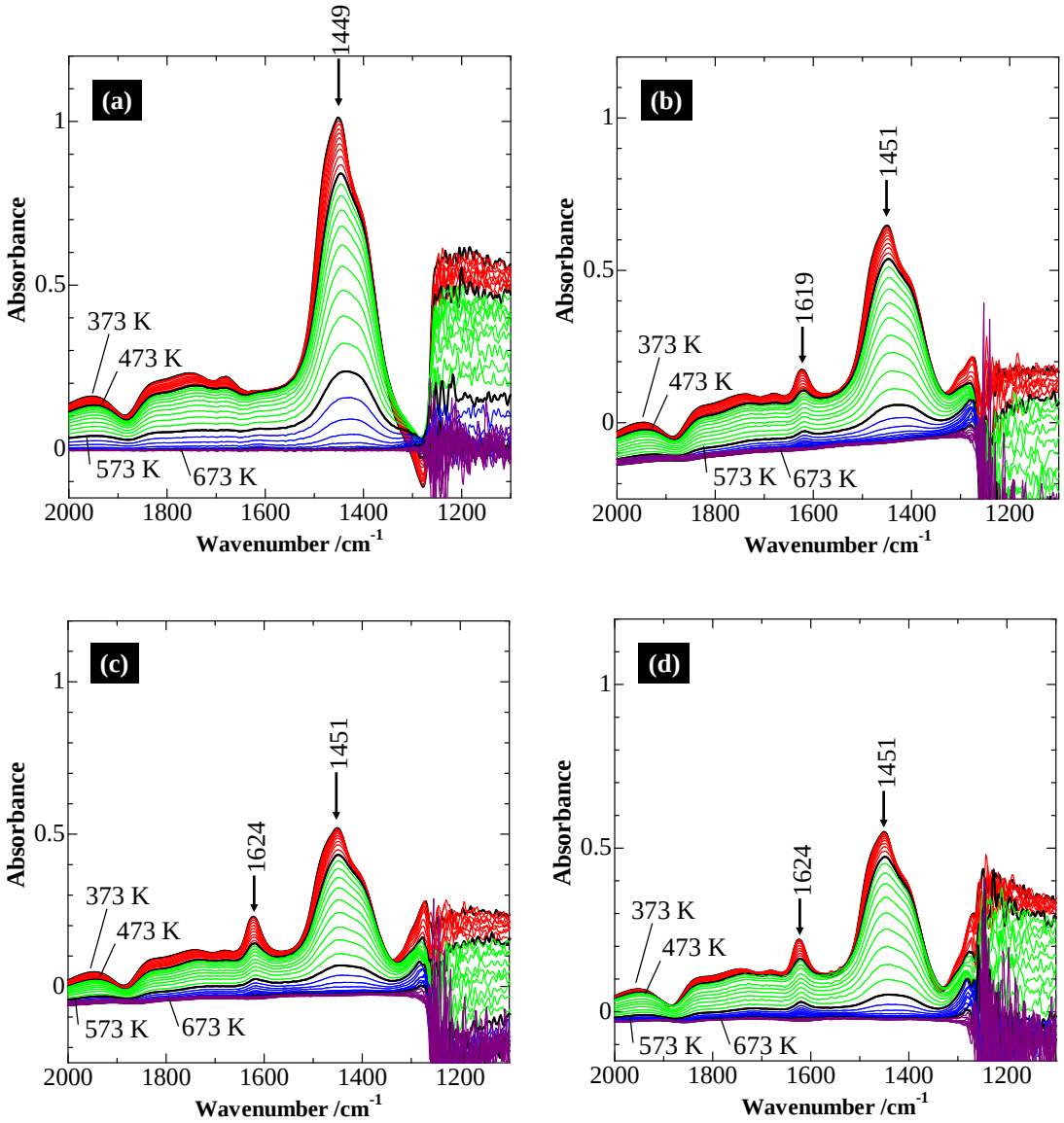
(a)
1449
373 K
473 K
573 K
673 K
Absorbance
Wavenumber /cm-1
(b)
1451
1619
373 K
473 K
573 K
673 K
Absorbance
Wavenumber /cm-1
(c)
1451
1624
373 K
473 K
573 K
673 K
Absorbance
Wavenumber /cm-1
(d)
1451
1624
373 K
473 K
573 K
673 K
Absorbance
Wavenumber /cm-1

Fig. 3

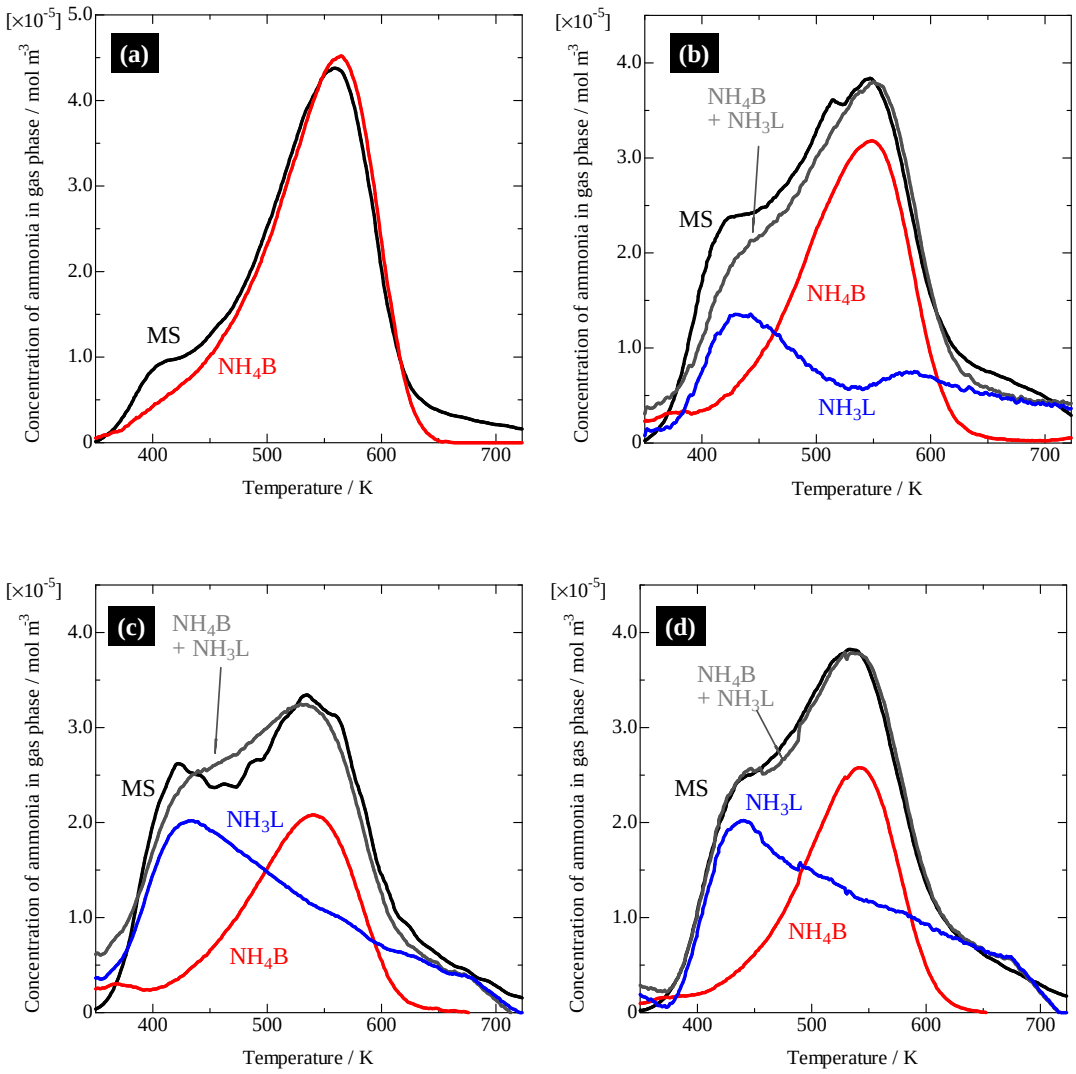
[×10-5]
Concentration of ammonia in gas phase / mol m-3
(a)
MS
NH4B
(b)
NH4B
+ NH3L
MS
NH4B
NH3L
(c)
NH4B
+ NH3L
MS
NH3L
NH4B
(d)
NH4B
+ NH3L
MS
NH3L
NH4B
Temperature / K

Fig. 4

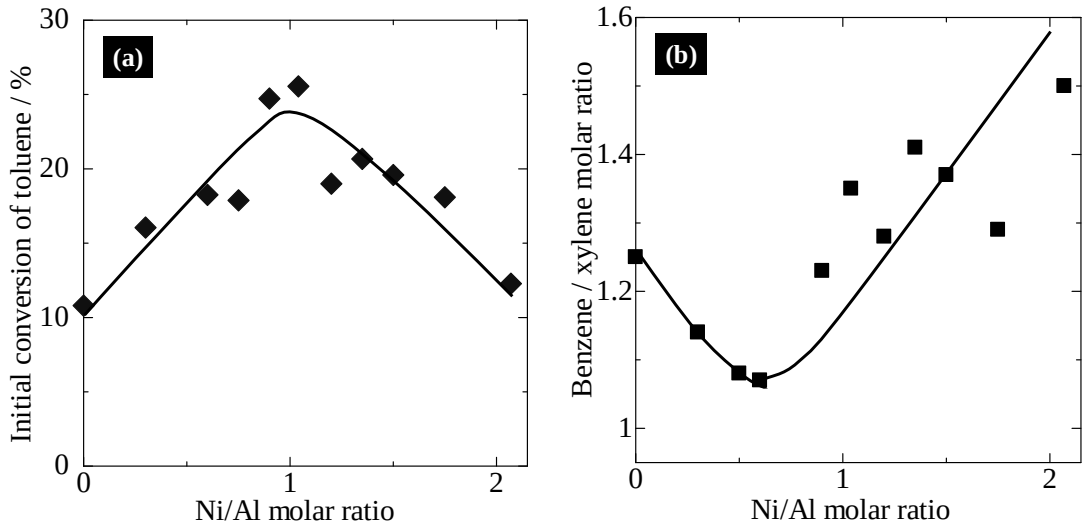
(a)
Initial conversion of toluene / %
Ni/Al molar ratio
0
10
20
30
0
1
2
(b)
Benzene / xylene molar ratio
Ni/Al molar ratio
1
1.2
1.4
1.6
0
1
2

Fig. 5

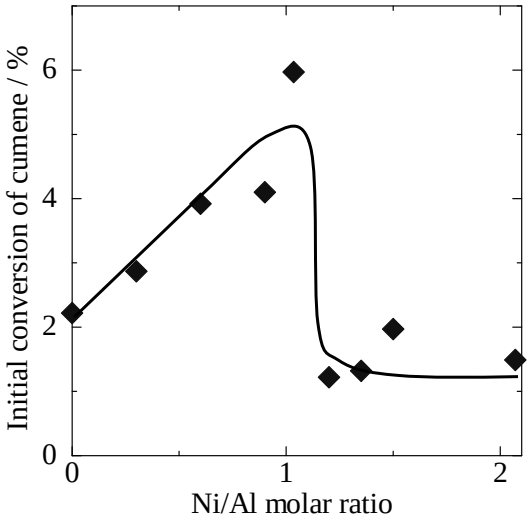

Fig. 6

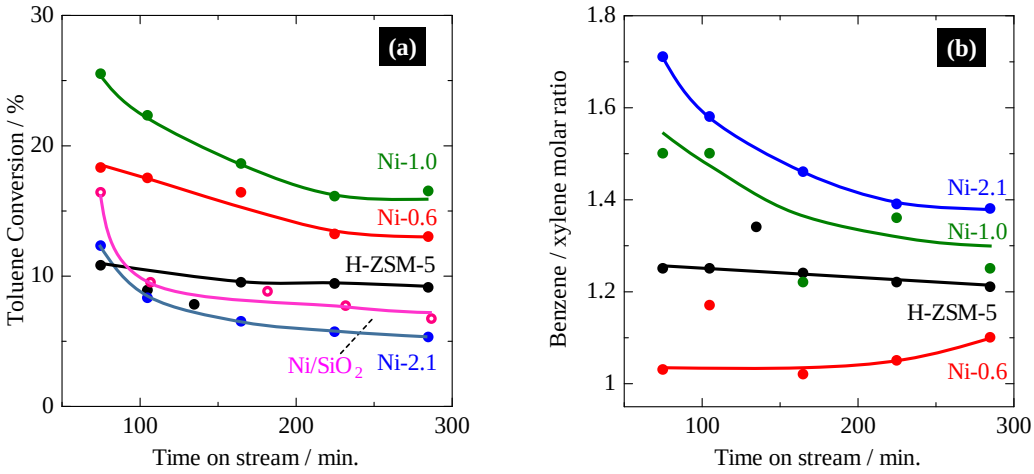
(a)
Toluene Conversion / %
Time on stream / min.
Ni-1.0
Ni-0.6
H-ZSM-5
Ni/SiO2
Ni-2.1
(b)
Benzene / xylene molar ratio
Time on stream / min.
Ni-2.1
Ni-1.0
H-ZSM-5
Ni-0.6

Fig. 7